CrystEngComm

Accepted Manuscript

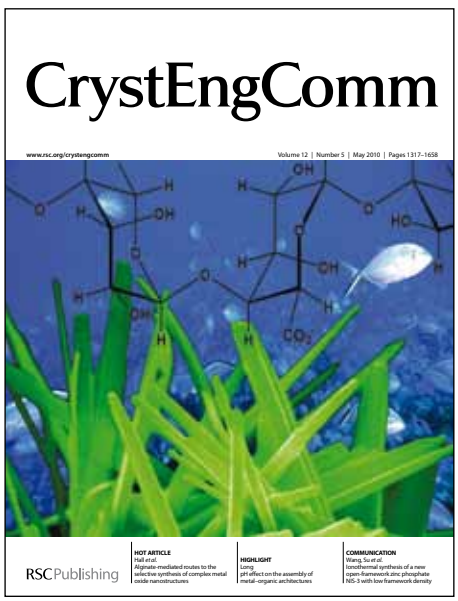

Submitted to the Special Theme issue of CEC on India IYCr Celebration

Pharmaceutical Cocrystals and a Nitrate Salt of Voriconazole

S. Sudalai Kumar, Ranjit Thakuria, and Ashwini Nangia*

School of Chemistry, University of Hyderabad, Central University PO, Prof. C. R. Rao Road, Gachibowli, Hyderabad 500 046, India

E-mail: ashwini.nangia@gmail.com

Abstract

Voriconazole ((2R,3S)-2-(2,4-difluorophenyl)-3-(5-fluoropyrimidin-4-yl)-1-(lH-l,2,4-triazol-l-yl)butan-2-ol, VZL) is an antifungal drug with low aqueous solubility of 0.71 mg/mL and it is a BCS class II drug (Biopharmaceutics Classification System) of the azole family. We have prepared a nitrate salt and three cocrystals of VZL with p-hydroxybenzoic acid, p-aminobenzoic acid (both are GRAS compounds) and m-nitrobenzoic acid coformers to improve the physicochemical properties. All four multi-component crystals of voriconazole were obtained by solution crystallization as well as solid-state grinding and their structures were confirmed by X-ray diffraction, FT-IR, Raman, and NMR spectroscopy, and thermal techniques. VZL–PHBA and VZL–PABA are isostructual by XPac calculations and molecular packing arrangement. A notable result from a crystal engineering viewpoint is that the supramolecular synthon between the basic drug and the acidic coformer undergoes a switch based on the pK_a of the acid.

† Electronic Supplementary Information available with this paper. Comparison of calculated and experimental PXRD plots (Fig. S1), FT-IR and Raman spectra (Fig. S2 and S3), PXRD plots of cocrystals and salt after slurry (Fig. S4), List of experiments for VZL solid forms search (Table S1), Hydrogen bonds in crystal structures (Table S2), ^{13}C chemical shift values in ppm (Table S3), and IR, Raman peaks (Table S4 and S5), CSD Refcodes (Table S6), and crystallographic .cif files (CCDC Nos. 971867-971870).

Introduction

Cocrystals are multi-component systems consisting of two or more neutral, solid compounds held together by hydrogen bonds in a definite stoichiometry.[1] To be a pharmaceutical cocrystal, one of the components (drug) must be an active pharmaceutical ingredient (API) and the other (coformer) should be a safe compound from the GRAS list (generally regarded as safe by the US-FDA).[2] The idea of preparing pharmaceutical cocrystals is to alter the physicochemical properties, most often solubility and dissolution rate, of a drug without modifying its chemical structure.[1,3] Itraconazole[4] and fluoxetine hydrochloride cocrystals[5] are early examples of pharmaceutical cocrystals, a trail that has been followed up with several hundred publications and several excellent reviews.[3] There are three examples of drug cocrystals in the market: caffeine-citric acid/citrate,[6a] and escitalopram-oxalic acid/oxalate, and valproic acid/Na-valproate.[6b,c] A few more cocrystals are in clinical stage.[6d]

Results and Discussion

Voriconazole (VFEND®, Pfizer) is an antifungal drug administered intravenously or in oral dosage formulation.[7] Two other antifungal drugs of the azole family, itraconazole and fluconazole, have been studied for salts, cocrystals and metal complexes.[4,8] A guest free form[9a] and a camphor sulfonate salt[9b] of voriconazole are reported along with nano-indentation study of the pure API.[9c] VZL has low aqueous solubility (0.71 mg/mL) and is unstable in water due to a retro-aldol reaction.[10] Due to the presence of less basic triazole and pyrimidine rings, voriconazole is able to form salts with strong acids only, whereas with moderate organic acids it can possibly form cocrystals[11] (Table 1). A complete list of coformers and crystallization experiments attempted is listed in Table S1 (ESI†). The successful nitrate salt and a few cocrystals are reported (Scheme 1) with the objective to analyze X-ray crystal structures and improve the physico-chemical profile of voriconazole.

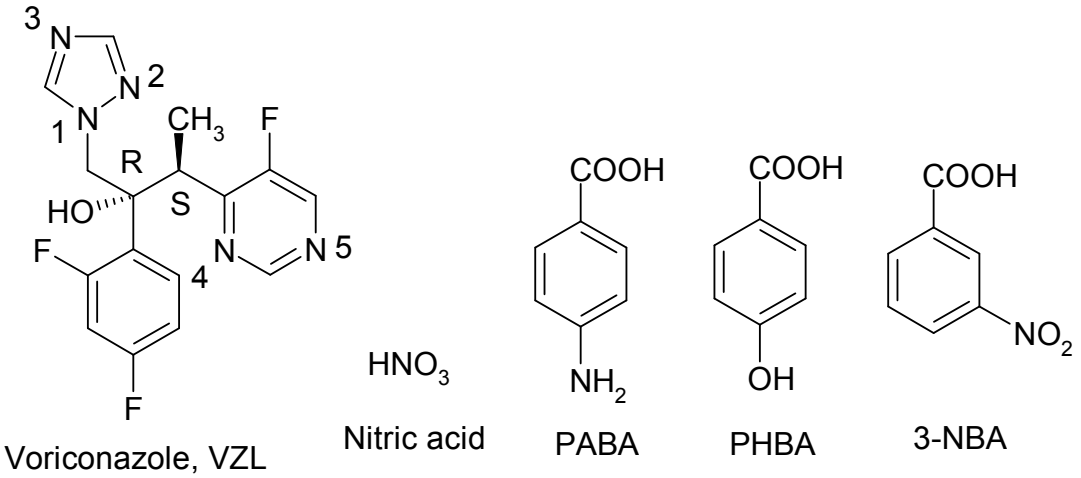

(a)

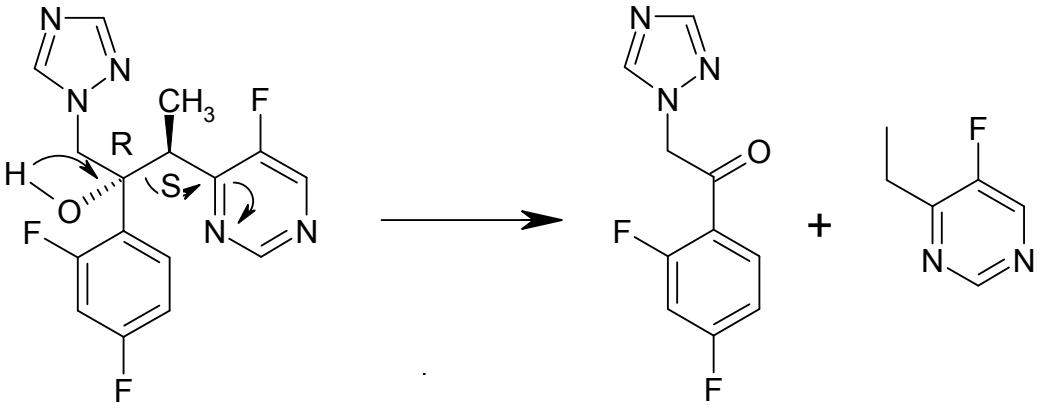

(b)

Scheme 1 (a) Voriconazole and successful coformers; (b) Retro-aldol degradation pathway of voriconazole in the aqueous medium.

Table 1 ΔpK_a value of voriconazole and coformers.

API/Coformer	pK_a[a]	Cocrystal/salt	ΔpK_a (COOH with N5- and N3-VZL)
VZL	2.27 (N3) 0.43 (N5)	-	-
HNO_3	–1.30	VZL–HNO_3	3.57, 1.73

PHBA	3.57 (COOH)	VZL–PHBA	–1.30, –3.14
PABA	4.87 (COOH)	VZL–PABA	–2.60, –4.44
3-NBA	3.49	VZL–3-NBA	–1.22, –3.06

[a] pK_a values for VZL are calculated from ChemAxon software. The pK_a values for VZL are those for the conjugate acid of the heterocycle N.

Structural analysis

Voriconazole dinitrate salt (1:2): Voriconazole dinitrate salt was prepared by dissolving 50 mg of voriconazole in 10 mL ethanol followed by the addition of 1-2 drops of 1N HNO_3 acid solution. The mixture was boiled for a few minutes and then kept for slow evaporation at ambient conditions. Colorless plate shaped crystals were obtained whose X-ray crystal structure was solved in the orthorhombic space group $P2_12_12_1$ with one voriconazolium and two nitrate ions in the asymmetric unit. Protons from two different nitric acid molecules are transferred to triazole N3 and pyrimidine N5 (partial transfer) of the voriconazole molecule. The fully ionized nitrate ion is sandwiched between the layers of voriconazole connected through bifurcated $N3^+$–H3A···$O2^-$ and $N3^+$–H3A···$O3^-$ (1.72 Å, 171° and 2.33 Å, 126°) hydrogen bonds (Table S2, ESI†) to make of graph set motifs of notation[12] $R_1^2(3)$ (Figure 1a). The second nitrate ion is connected to N5 pyrimidine through $N5^+$–H6A···$O6^-$ interaction and a second molecule of voriconazole through weak van der Waal interactions in a zigzag tape (Figure 1b).

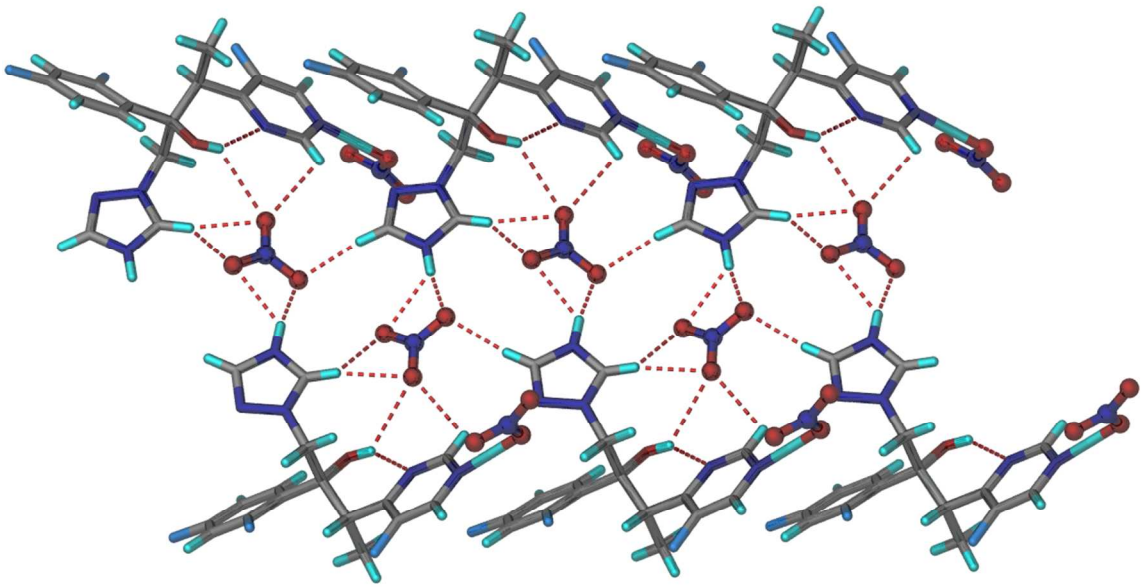

(a)

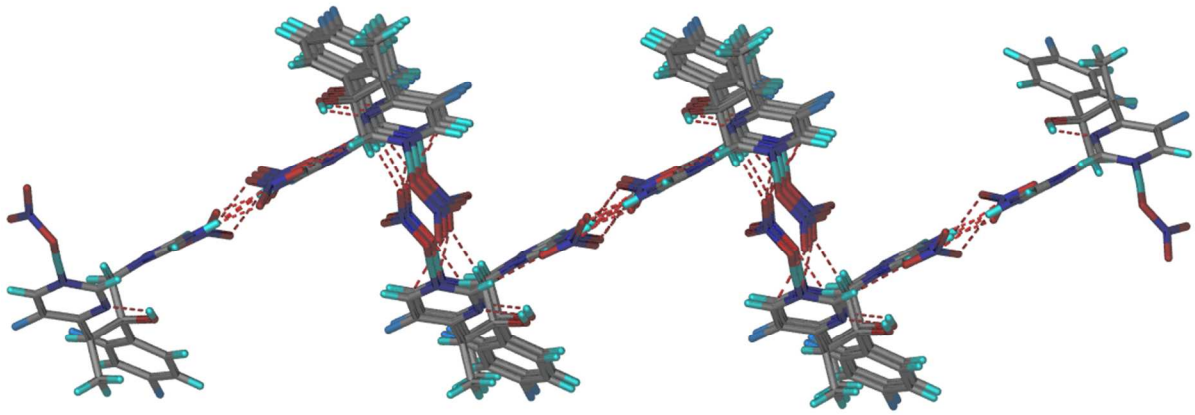

(b)

Figure 1 (a) Nitrate ions form strong ionic N^{+}–H···O^{-} and weak C–H···O hydrogen bonds with voriconazole molecules, and (b) C–H···O hydrogen bonds in the zigzag tapes of VZL molecules connected via nitrate ions.

Voriconazole–p-hydroxybenzoic acid (1:1): VZL–PHBA 1:1 cocrystal was prepared by mixing the components (0.30 mmol each) in 10 mL methanol and kept for slow evaporation. Colorless plate-shape crystals were solved in the monoclinic space group $P2_1$. VZL and PHBA are connected in a helical chain through O–H···N hydrogen bonds (Figure 2). The carboxyl group of PHBA forms a two-point synthon with the pyrimidine N5 of VZL rather than the N3 of triazole. The p*K*a values of the two N positions suggest a strong hydrogen bond between the carboxylic acid donor and N3 of triazole as acceptor based on ΔpK_a (Table 1). The triazole N3 (pK_a of conjugate acid 2.72) is a stronger base than pyrimidine N5 (pK_a NH^{+} 0.43). Etter's rule[12a,b] of strong hydrogen bond donor–acceptor pairing does not seem to be followed in this system. The tertiary OH group pK_a is very high (12.71) for any kind of ionization at physiological conditions. The hydroxyl group of PHBA forms O–H···N hydrogen bond to triazole N3.

Voriconazole is a multiple acidic/basic site molecule, and accurately determining the pK_a of each N atom is very difficult. A survey of the literature afforded two different sets of pK_a values for voriconazole. Buchanan et al.[13a] reported 4.98 and 12.0, and Reddy et al.[13b] reported 2.72 and 11.54. It is clear that the higher value of 11-12 refers to the OH group pK_a.[13c] It was not

mentioned in the above papers whether the 2nd pK_a number refers to that of azole N or the pyrimidine N. We then searched the pK_a of a related azole drug without the pyrimidine ring, and the values for fluconazole are 11.01, 2.94, 2.65.[13d] Therefore the value of 2.72 taken for triazole N is the correct assignment. The pyrimidine N basicity may be severely attenuated by the meta-fluoro group and so triazole N is the more basic site in voriconazole.

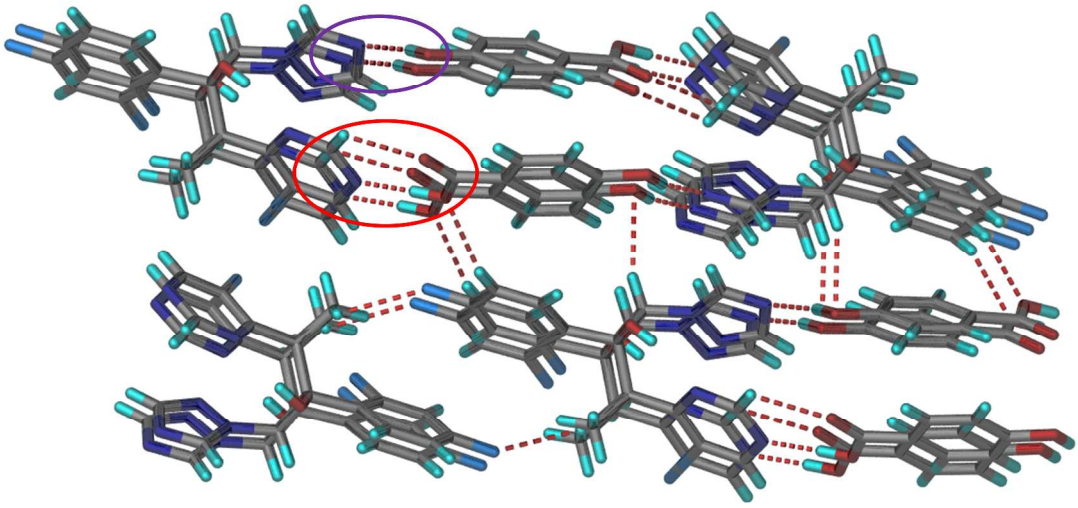

Figure 2 VZL forms strong O−H···N and weak C−H···O hydrogen bonds with PHBA.

Voriconazole–p-aminobenzoic acid (1:1): VZL–PABA cocrystal was crystallized from a 1:1 solution of methanol and ethanol. The colorless plates of VZL–PABA 1:1 cocrystal were solved in the monoclinic space group $P2_1$ with a helix of VZL and PABA connected via O−H···N and N−H···N hydrogen bonds (Figure 3). Similar to the VZL–PHBA, VZL–PABA also is assembled via carboxylic acid-pyrimidine two-point synthon and one-point N−H···N hydrogen bond between the amino group of PABA and triazole N3 of VZL.

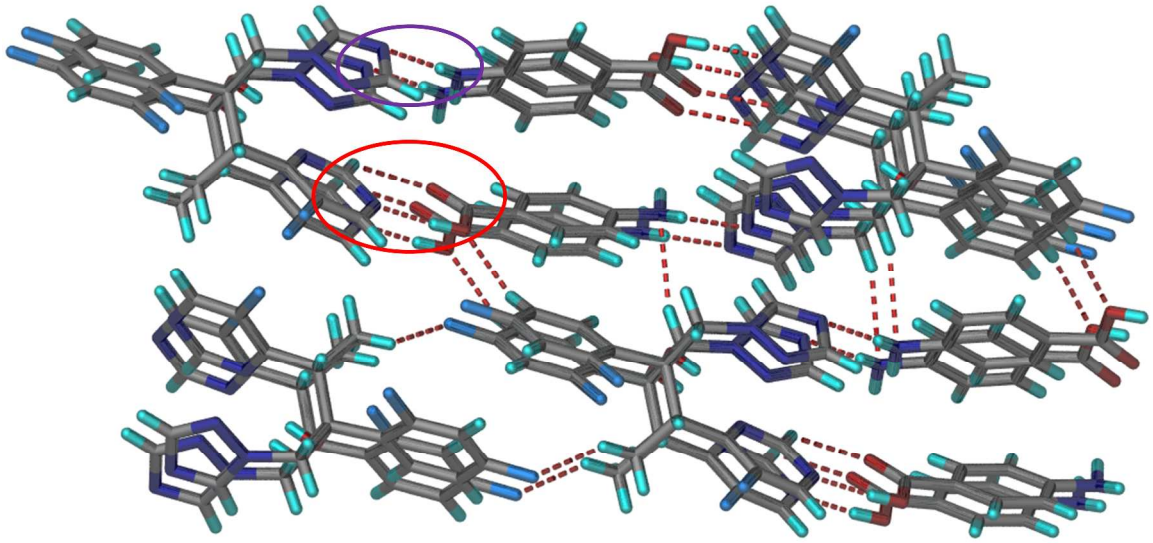

Figure 3 The strong acid-pyrimidine two-point synthon and amino-triazole one-point synthon is shown along with weak interactions between VZL and PABA.

The structures of VZL–PHBA and VZL–PABA have similar hydrogen bond motifs with O−H/ N−H exchange for the coformers PHBA and PABA. They are isomorphous structures (Table 2). The isostructurality of single component and multi-component systems (cocrystals, solvates, and complexes) by chloro-methyl, C−H/ N−H, N−H/ O−H, C−H/ O−H, halogen exchange are well represented.[14] The XPac dissimilarity[15] index value of 2.9 (a small number) is indicative of 3D isostructurality between PHBA and PABA cocrystals of VZL (Figure 4).

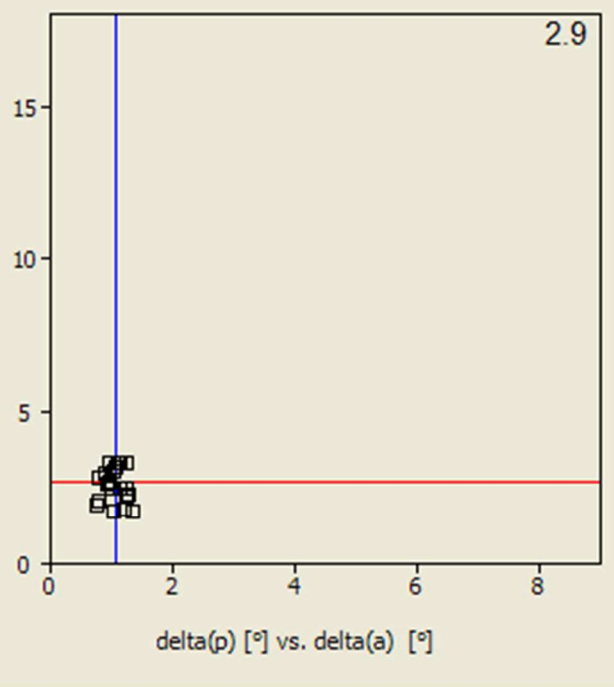

(a)

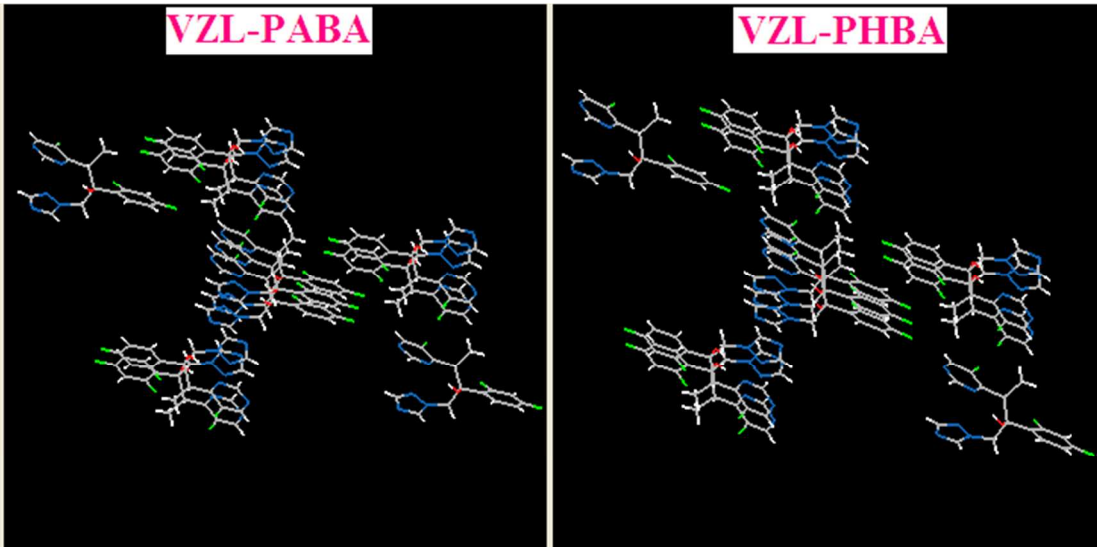

(b)

Figure 4 (a) The XPac dissimilarity index of 2.9 indicates similarity between PHBA and PABA cocrystals, (b) 3D supramolecular construct in VZL–PABA and VZL–PHBA.

4. Voriconazole–3-nitrobenzoic acid (1:1): VZL–3-NBA 1:1 cocrystal was prepared by dissolving a 1:1 mixture of voriconazole (100 mg) and 3-nitrobenzoic acid (48 mg) in

acetonitrile and kept for slow evaporation at ambient conditions. Thin plate shaped colorless crystals were solved in the monoclinic space group $P2_1$. The carboxylic acid group of 3-NBA is hydrogen bonded to triazole N3 via O−H···N and C−H···O two-point synthon, consistent with Etter's[12] hydrogen bond pairing rule (Figure 5). The O−H donor of VZL makes bifurcated H bonds with N4 of pyrimidine (intramolecular hydrogen bond) and triazole N2 of the next molecule in an infinite chain.

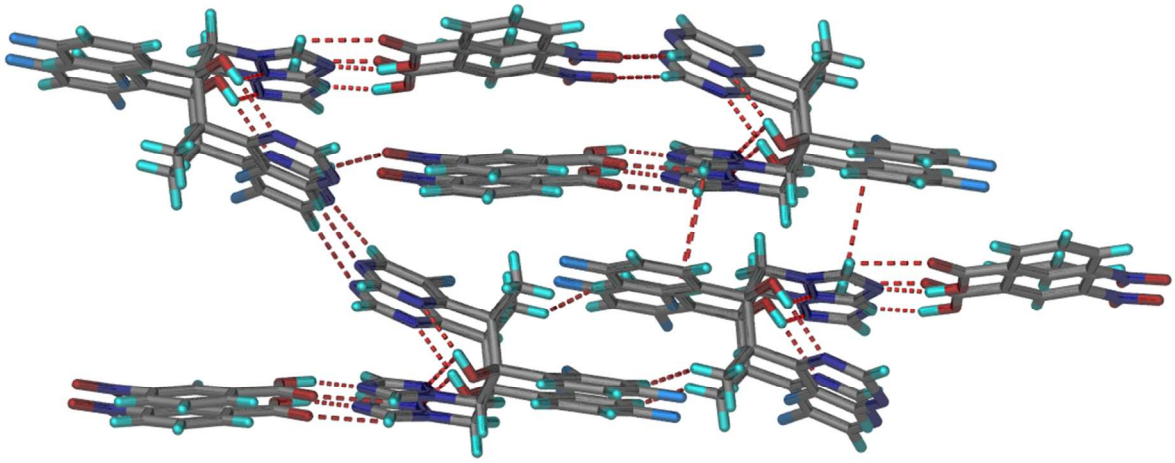

Figure 5 The triazole ring of VZL forms strong O−H···N and weak C−H···O hydrogen bonds with 3-NBA.

Table 2 Crystallographic detail of VZL complexes

Compound	VZL–HNO_3	VZL–PHBA	VZL–PABA	VZL–3-NBA	VZL
Solid forms	Salt	Cocrystal	Cocrystal	Cocrystal	Ref 9a
Empirical formula	$C_{16}H_{16}F_3N_7O_7$	$C_{23}H_{20}F_3N_5O_4$	$C_{23}H_{21}F_3N_6\ O_3$	$C_{23}H_{19}F_3N_6O_5$	$C_{16}H_{14}F_3N_5O$
Formula weight	475.36	487.44	486.46	516.44	349.32
Crystal system	Orthorhombic	Monoclinic	Monoclinic	Monoclinic	Monoclinic
Space group	$P2_12_12_1$	$P2_1$	$P2_1$	$P2_1$	$P2_1$
a (Å)	9.1515(9)	13.7102(5)	13.674(11)	11.5743(5)	7.5332 (19)
b (Å)	13.1275(13)	6.04623(17)	6.085(5)	6.7286(2)	8.349 (2)
c (Å)	16.1908(16)	14.2265(5)	14.196(11)	14.9073(6)	12.989 (3)
α (°)	90	90	90	90	90
β (°)	90	107.314(4)	106.543(12)	97.526(4)	100.062 (4)

γ (°)	90	90	90	90	90
V (Å^3)	1945.1(3)	1125.87(7)	1132.4(15)	1150.96(8)	804.4 (3)
Dcalcd (g cm^{-3})	1.623	1.438	1.427	1.490	1.442
μ (mm^{-1})	0.147	0.117	0.114	0.124	0.12
θ range (º)	2.00-26.06	2.93- 24.96	2.44-22.71	2.75-26.31	25.0
Z/Z′	4/1	2/1	2/1	2/1	--
Range h	-11 to 11	-16 to 10	-16 to 16	-13 to 14	--
Range k	-16 to 16	-6 to 6	-7 to 7	-7 to 8	--
Range l	-19 to 19	-16 to 16	-17 to 17	-18 to 17	--
Reflections collected	20312	3814	11761	5175	7364
Observed reflections	3830	3071	4474	3868	1529
Total reflections	3753	2831	3718	2649	1398
R1 [I > 2 σ(I)]	0.0305	0.0345	0.0540	0.0384	0.0509
wR2 (all)	0.0768	0.0933	0.1123	0.0750	-
Goodness-of-fit	1.059	1.086	1.137	0.911	-
T (K)	100	298	298	298	294
X-ray diffractometer	Bruker SMART APEX	Oxford Xcalibur Gemini	Bruker SMART APEX	Oxford Xcalibur Gemini	Bruker SMART APEX

Supramolecular synthon and CSD search:

From the four crystal structures and the reported sulphonate salt it was observed that there is a synthon switch depending on the pK_a value of the coformer. The strongly acidic 3-NO_2-PhCOOH preferentially forms the acid−triazole synthon (eg. VZL–3-NBA cocrystal) whereas weaker acids make the acid-pyrimidine synthon (e.g. as in VZL–PHBA and VZL–PABA). Both types of heterosynthons are two-point and assembled via O–H···N and C–H···O hydrogen bonds, and so it difficult to rationalize this switch. The very strong nitric acid gives a dinitrate with both azole and pyrimidine N being protonated. A search of the Cambridge Structural Database[16a] for carboxylic acid−pyrimidine and acid−triazole two-point synthon gave only 2 hits for acid−triazole and 5 hits for acid−pyrimidine (Scheme 2 and Table 3). The number of archived

crystal structures with the given motif is too small to extract a pK_a dependent synthon trend. Related searches on protonated triazole and acid−triazole single O−H···N hydrogen bond gave 38 and 18 hits respectively (see details in Table S5, ESI†). The difficulty in making cocrystals of azole drugs with COOH is contrary to pK_a prediction, but nonetheless a fact known from the literature,[4,9b] and the few CSD hits (Table 3).

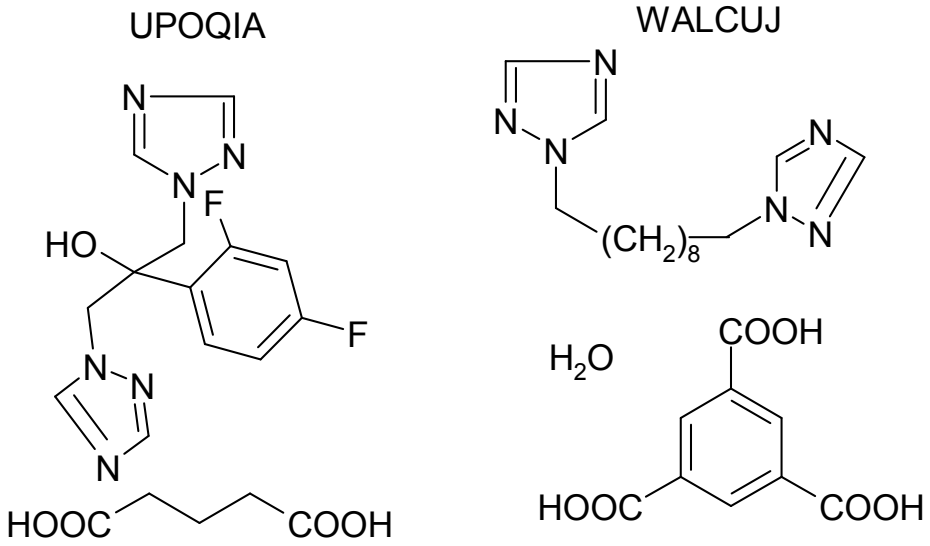

Scheme 2 Chemical structures of CSD Refcodes with acid–triazole two-point O–H···N and C–H···O synthon.

Table 3 CSD refcodes for the acid−traiazole synthon and calculated pK_a values.[a]

Carboxylic acid–triazole two-point synthon (2 hits)	pK_a of triazole nitrogen (NH^+) and acid	ΔpK_a (= NH^+ – acid)
UPOQIA	2.03, 4.32	–2.29
WACLUJ	1.99, 4.55	–2.56
Carboxylic acid–pyrimidine two-point synthon (5 hits)	pK_a of pyrimidine nitrogen (NH^+) and acid	ΔpK_a (= NH^+ – acid)
ABIWIT	1.78, 3.15	–1.57
POFPEF	1.58, 4.14	–2.56
XAQNOT	–0.28, 3.80	–4.08
LEJMOE	1.99, 4.37	–2.38
TENSIQ	1.19, 4.37	–3.18

[a] pK_a values are calculated from ChemAxon software

Conformation of VZL

The presence of flexible methylene group between the heterocycle ring and the chiral center results in two clusters of conformations for voriconazole in the solid-state (Figure 6). The free base and the dinitrate salt have a similar conformation whereas the cocrystals overlay in a different orientation for the triazole ring (see Table 4 for torsion angles).

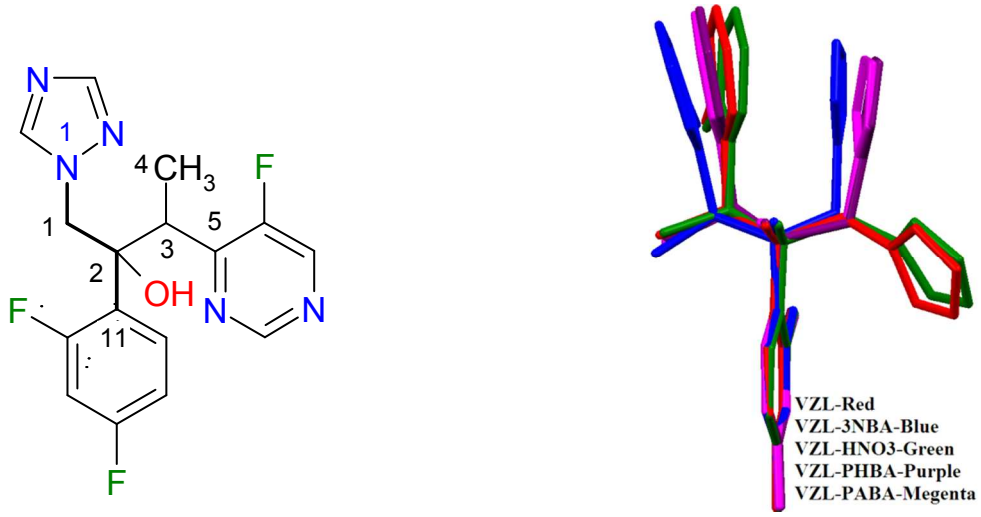

(a) (b)

Figure 6 (a) Molecular structure of VZL with atom labeling considered for conformation analysis, and (b) Molecular overlay of different conformers of VZL in crystal structures.

Table 4 Torsion angle values of voriconazole salt and cocrystals.

Solid forms	Torsion angle (°) τ_1 (C11−C2−C1−N1)	Torsion angle (°) τ_2 (C11−C2−C3−C5)	Torsion angle (°) τ_3 (C1−C2−C3−C4)
VZL (ref 9a)	55.6(4)	175.6(3)	175.0(3)
VZL–HNO_3	61.7(2)	179.6(1)	179.8(1)
VZL–PHBA	173.4(2)	168.4(2)	164.6(2)
VZL–PABA	170.5(2)	169.1(2)	165.2(2)
VZL–3-NBA	175.18(19)	169.3(2)	167.5(2)

Characterization of VZL crystalline forms

Voriconazole salt and cocrystals were prepared for spectroscopic and thermal characterization by neat and liquid assisted grinding (LAG).[16b] The PXRD of the materials match well with the calculated powder pattern from the crystal structure (Fig S1, ESI†). ^{13}C ss-NMR,

FT-IR, FT-Raman (Fig S2-S3, ESI†) and differential scanning calorimetry (DSC) confirmed the bulk purity of the crystalline products (Table S3-S5, ESI†).[16c,d,e]

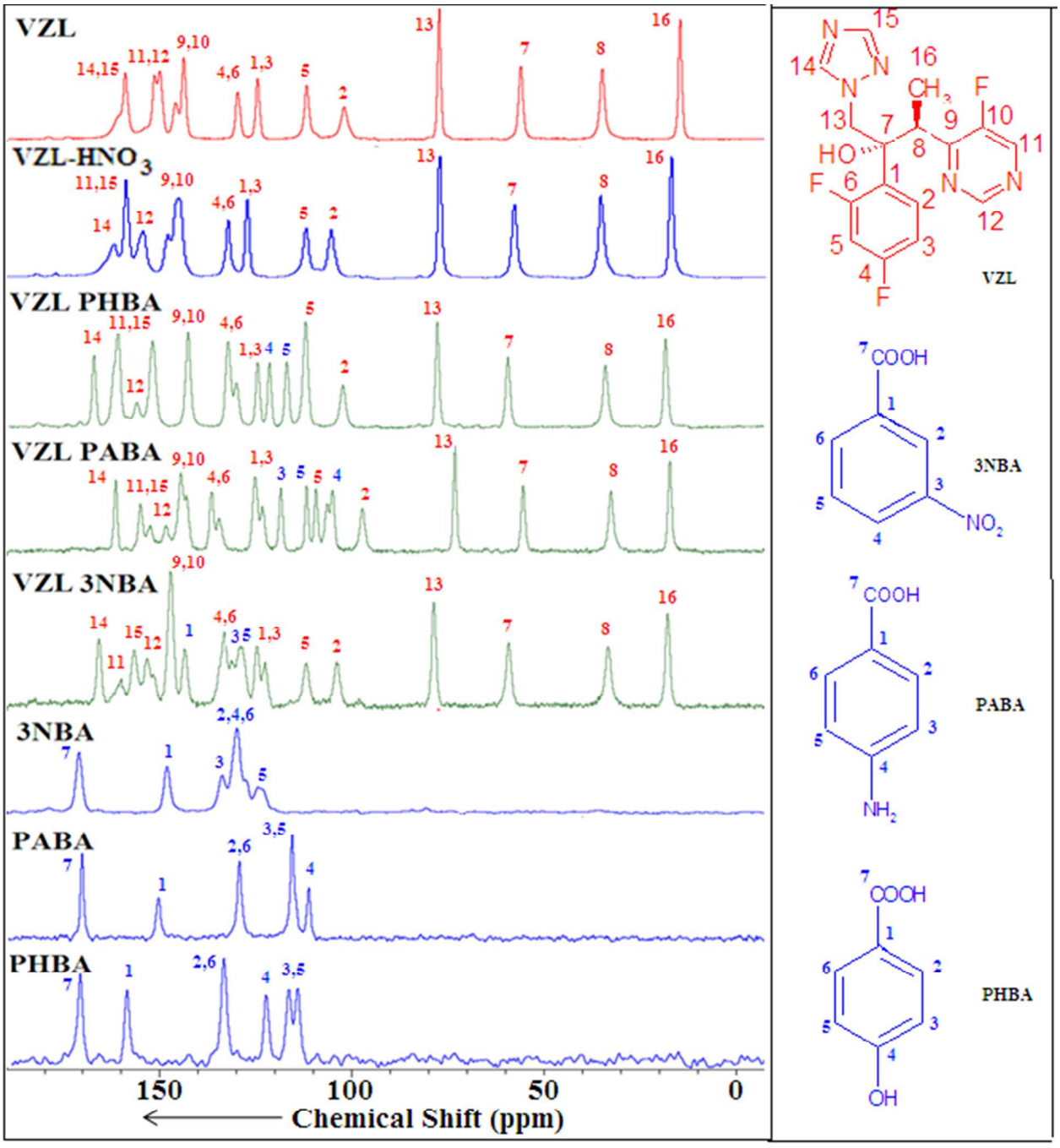

Figure 7 ^{13}C ss-NMR spectra of VZL dinitrate salt and cocrystals.

Thermal analysis confirms the formation of VZL salt and cocrystals. Though VZL–PABA and VZL–PHBA are isomorphous, there is a large difference in their melting points (152

°C, 120 °). This difference might be due to the presence of two hydrogen bond donors in p-aminobenzoic acid that has the additional hydrogen bond (N6−H6A···O3) in the crystal structure of VZL−PABA with a molecule in the adjacent layer compared to VZL-PHBA which lacks this stabilizing interaction. Their crystal density is comparable (VZL−PHBA 1.43 g cm^{-3}, VZL−PABA 1.42 g cm^{-3}). The similarity in the molecular confirmation of these two isostructural cocrystals suggests that the additional interaction in VZL−PABA is responsible for the higher in the melting point. VZL–3-NBA has a low melting point of 95 °C. The conformation of this cocrystal is slightly different from other two cocrystals of PABA and PHBA in the overlay of molecular conformations[17] (Figure 6). Molecular conformation and melting point of carboxylic acids have been correlated in the recent literature.[18] DSC thermograms of VZL complexes are shown in Figure 8. The dinitrate salt melts at 151° C and the large exotherm in DSC indicates decomposition of the salt at 154° C.

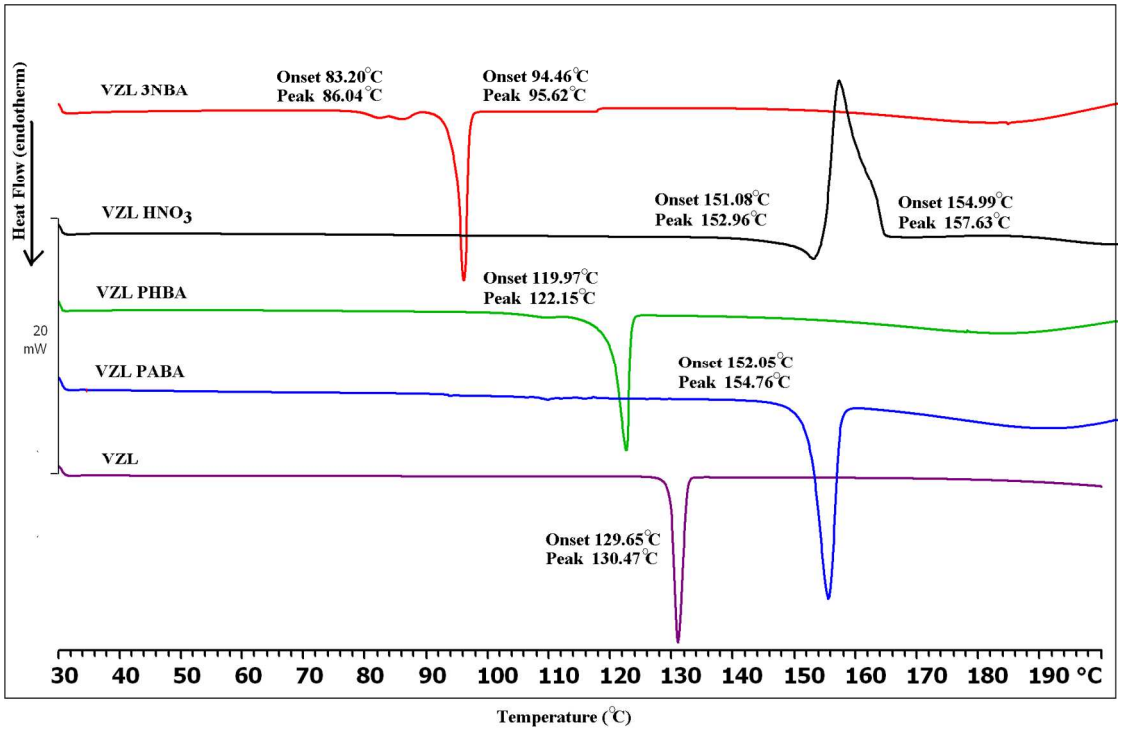

Figure 8 DSC of VZL adducts.

Table 5 Melting temperatures of solid forms of VZL

Solid forms	m.p. of	m.p. of	Density

	cocrystal/salt (°C)	Coformers (°C)	(g cm^{-3})
VZL	129.6	-	1.442
VZL–HNO_3	151.0	-	1.623
VZL–PHBA	119.9	215	1.438
VZL–PABA	152.0	188	1.427
VZL–3-NBA	94.46	140	1.490

Solubility and Dissolution study

Solubility and dissolution behavior of voriconazole salt and cocrystals were measured in 0.1 N HCl. The advantage of salt preparation with respect to cocrystal is well established in the literature.[19] However, due to the presence of less basic groups (N3 of triazole and N5 of pyrimidine) in voriconazole, salt preparation is difficult and proton transfer occurred only with the strong HNO_3. The dinitrate salt of voriconazole is about 10 times more soluble (2.5 mg/ mL) than the free base (0.26 mg/ mL) in 0.1 N HCl. The cocrystals with EAFUS coformers[2] (PABA and PHBA) and 3-NBA have lower solubility (1.16, 0.35 and 0.39 mg/ mL). It is noteworthy that the isomorphous VZL–PABA cocrystal is ~ 3 times more soluble than VZL–PHBA. The reason for the higher solubility of PABA cocrystal is due to the higher solubility of the coformer PABA (6.11 mg/mL) compared to PHBA (4.89 mg/mL) and the presence of NH_2 (two H-bond donors) compared to OH (one H-bond donor) group, which will lead to greater hydration in solution.[20]

The intrinsic dissolution[21] data follows similar trends (Table 6). The nitrate salt has ~ 3 times faster IDR compared to VZL base (Figure 9). The materials were found to be stable as confirmed by PXRD of the residue at the end of the solubility and dissolution measurements (Figure S4, ESI†).

Table 6 Solubility and Intrinsic dissolution rate of VZL solid forms

Solid forms	λ_{max} (nm)	Absorption coefficient (ε), (M^{-1} cm^{-1})	IDR in 0.1N HCl (x10^{-2} mg/cm^2)	Solubility in 0.1N HCl (mg/mL)
VZL	257	318.37	3.27	0.26
VZL–HNO_3	259	141.91	9.18	2.57
VZL–PHBA	258	547.70	3.86	0.35
VZL–PABA	257	187.05	5.20	1.16

VZL–3-NBA	258	337.13	3.95	0.39

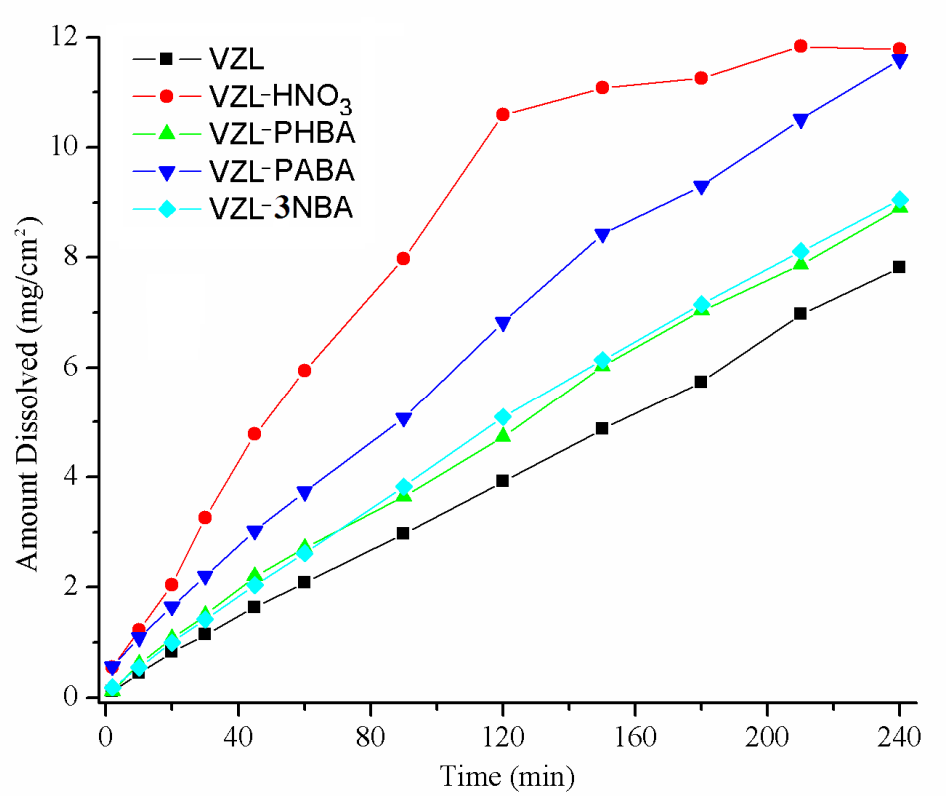

Figure 9 Dissolution profile of voriconazole pure base and its solid forms in 0.1N HCl solution in 4 h.

Conclusions

A nitrate salt and three cocrystals of voriconazole with PHBA, PABA and 3-NBA were prepared in bulk as well by solution crystallization. All the multi-component structures of voriconazole were characterized using solid-state characterization techniques. Overall, the success rate for cocrystal/ salt formation was found to be very difficult from the 30 or so conformers/ salt formers attempted. From the solved crystal structures it was observed that there is a synthon switch from acid−pyrimidine to acid−triazole synthon depending on the strength of the coformer acid. The weaker PABA and PHBA are sustained by acid−pyrimidine whereas stronger 3-NBA cocrystal contains acid−triazole synthon. Both the pyrimidine and triazole N are protonated in the dinitrate salt. The occurrence of these synthons is compared with CSD statistics. There are very few reports for these two synthons and the present analysis adds

structural data to the less known acid–triazole and acid–pyrimidine two-point synthons. The isostructurality between PHBA and PABA cocrystals of voriconazole was quantified by XPac. The good solubility and dissolution of VZL–PABA cocrystal is encouraging along with the dinitrate salt of voriconazole for formulation development.

Experimental Section

Materials

Voriconazole was purchased from Shanghai Xunxin Chemical Co., Ltd., China and was used without any further purification. All other coformers were of analytical or chromatographic grade and were purchased from Sigma-Aldrich (Hyderabad, India). Water altered through a double-deionized purification system (Milli Q Plus Water System from Millipore Co., Billerica, Massachusetts) was used in all the experiments. Melting points were measured on a Fisher-Johns melting point apparatus. Single crystals were obtained via slow evaporation of stoichiometric amounts of starting materials in appropriate organic solvents after solid state and liquid assisted grinding in a mortar-pestle. Cocrystals and salt were characterized by FT-IR, Raman, ^{13}C ss-NMR spectroscopy techniques, DSC, PXRD and single crystal X-ray diffraction (SC-XRD).

Preparation of cocrystals by liquid (solvent drop) assisted grinding

1. Voriconazole (VZL)

Voriconazole crystals were obtained from organic alcoholic solvents and the ground material of these crystals was used in the comparison of analysis and characterizations with the new solid forms. m.p. 130-132 °C.

2. VZL–PHBA (1:1) cocrystal

100 mg (0.28 mmol) voriconazole and 38.5 mg (0.28 mmol) p-hydroxybenzoic acid were ground in mortar-pestle for 15 min after adding 5 drops of EtOH, and then kept for crystallization in 10 mL ethanol. Suitable plate type crystals appeared at ambient condition after 3-4 days. m.p. 120-122 °C.

3. VZL–PABA (1:1) cocrystal

100 mg (0.28 mmol) voriconazole and 39.2 mg (0.28 mmol) p-aminobenzoic acid were ground in mortar-pestle for 15 min after adding 5 drops of EtOH, and then kept for crystallization in 10 mL ethanol. Suitable thick plate crystals were harvested at ambient condition after 3-4 days. m.p. 150-153 °C.

4. VZL−3NBA (1:1) cocrystal

100 mg (0.28 mmol) voriconazole and 47.8 mg (0.28 mmol) PABA was ground in mortar-pestle for 15 min after adding 5 drops of EtOH/CH_3CN, and then kept for crystallization in 10 mL ethanol. Suitable block and plate type crystals were harvested at ambient condition after 3-4 days. m.p. 94-96 °C.

5. VZL–HNO_3 (1:2) salt

100 mg (0.28 mmol) voriconazole is dissolved in 10 mL of ethanol and boiled on a hot plate to reach the homogeneous solution. Few drops of diluted nitric acid solution is added into the homogeneous solution of voriconazole, boiled for 2-3 minutes and allowed for evaporation under room temperature condition. Suitable plate type crystals were harvested at ambient condition after 3-4 days. m.p. 152-154 °C.

X-ray Crystallography. X-ray reflections for voriconazole dinitrate salt (LT data) and voriconazole:p-hydroxybenzoic acid (RT data) were collected on a Bruker SMART APEX CCD diffractometer equipped with a graphite monochromator and Mo-Kα fine-focus sealed tube (λ = 0.71073 Å). Data integration was done using SAINT.[22a] Intensities for absorption were corrected using SADABS. [22b] Structure solution and refinement were carried out using Bruker SHELX-TL.[22c] X-ray reflections for voriconazole:p-aminobenzoic acid and voriconazole:3-nitrobenzoic acid (RT data) were collected on an Oxford Xcalibur Gemini Eos CCD diffractometer using Mo-Kα, radiation. Data reduction was performed using CrysAlisPro (version 1.171.33.55).[22d] OLEX2-1.0 and SHELX-TL 97 were used to solve and refine the data.[22e] All non-hydrogen atoms were refined anisotropically, and C−H hydrogens were fixed. In case of VZL-HNO_3, the N–H location in pyimidine ring was not stable in mapping as the proton is only partially protonated from HNO_3 to the pyrimidine ring. The reason for this partial proton transfer is due to the less basic nature of pyrimidine N compared to triazole. O–H and N–H protons were located from difference electron density maps and C–H hydrogens were fixed. Hydrogen bond distances were neutron normalized using WingGX-PLATON.[22f] Packing diagrams were prepared in X-Seed.[22g] Crystallographic .cif files (CCDC Nos. 971867-971870) are available at www.ccdc.cam.ac.uk/data_request/cif or as part of the Supporting Information.

CSD Search. All organic compounds, with "triazole" and pyrimidine" with the intermolecular distance of 1-3 Å with "carboxylic acid" in the qualifier, and entries for which 3D coordinates are determined were searched in Cambridge Structural Database, ver. 5.34, ConQuest 1.15,

November 2012 release, May 2013 update. Two hits for triazole−carboxylic acid and five hits for pyrimidine−carboxylic acid two point synthon of O−H···N and C−H···O hydrogen bonds were retrieved. The combination search of both triazole and pyrimidine synthons in the same distance range with carboxylic acid gave 0 hits. These data and Refcodes for CSD search are summarized in Table 3.

Vibrational Spectroscopy. Nicolet 6700 FT-IR spectrometer with an NXR FT-Raman module was used to record IR spectra. IR spectra were recorded on samples dispersed in KBr pellets. Raman spectra were recorded with the pellet of samples.

^{13}C ss-NMR Spectroscopy. Solid-state NMR spectra were recorded on a Bruker Advance spectrometer operating at 400 MHz (100 MHz for ^{13}C nucleus). ss-NMR spectra were recorded on a Bruker 4 mm double resonance CP-MAS probe in zirconia rotors at 5.0 kHz spin rate with a cross-polarization contact time of 2.5 ms and a recycle delay of 8 s. ^{13}C CP-MAS spectra recorded at 100 MHz were referenced to the methylene carbon of glycine and then the chemical shifts were recalculated to the TMS scale ($\delta_{glycine}$ = 43.3 ppm).

Thermal Analysis. DSC was performed on Mettler Toledo DSC 822e module. Samples were placed in crimped but vented aluminum sample pans. The typical sample size was 3-4 mg, and the temperature range was 30-200°C at heating rate of 5 °C/min. Samples were purged by a stream of dry nitrogen flowing at 150 mL/min.

Dissolution and Solubility Measurements. Intrinsic dissolution rate (IDR) and solubility measurements were carried out on a USP certified Electrolab TDT-08 L dissolution tester (Electrolab, Mumbai, MH, India). A calibration curve was obtained for all the solid forms by plotting absorbance vs. concentration UV-vis spectra curves on a Thermo Scientific Evolution EV300 UV-vis spectrometer (Waltham, MA) for known concentration solutions in 0.1N HCl solutions medium. The slope of the plot from the standard curve gave the molar extinction coefficient (ε) by applying the Beer-Lambert's law. Equilibrium solubility was determined in 0.1N HCl solutions medium using the shake-flask method. To obtain equilibrium solubility, 15-200 mg of each solid material was stirred for 24 h in 5-10 mL of 0.1N HCl solutions at 37 °C, and the absorbance was measured at 257-260 nm. The concentration of the saturated solution was calculated at 24 h, which is referred to as the equilibrium solubility of the stable solid form. The dissolution rates are obtained from the IDR experiments.

Powder X-ray Diffraction. PXRDs were recorded on a SMART Bruker D8 Advance X-ray diffractometer (Bruker-AXS, Karlsruhe, Germany) in the Bragg-Brentano geometry using Cu-Kα X-radiation (λ = 1.5406 Å) at 40 kV and 30 mA. Diffraction patterns were collected over the 2θ range of 5-50° at a scan rate of 1°/min. The appearance of new solid phases was monitored by the appearance of new diffraction peaks when comparing with the starting materials. Powder Cell 2.359[21h] was used for overlaying the experimental XRPD pattern on the calculated lines from the crystal structure.

Melting Point. Fisher-Scientific instrument is used for the determination of melting points of VZL and its solid forms. Samples were taken in less than 1 mg quantity for this study.

Acknowledgement: This research was funded by J. C. Bose fellowship (SERB-DST SR/S2/JCB-06/2009), research scheme Novel solid-state forms of APIs (SERB-DST SR/S1/OC-37/2011), and Pharmaceutical Cocrystals (CSIR 01-2410/10/EMR-II). DST (IRPHA) and University Grants Commission (UGC-PURSE grant) are thanked for providing instrumentation and infrastructure facilities. SSK and RT thank the CSIR and UGC for fellowship and contingency grant.

References

1. (a) D.-K. Bučar, G. M. Day, I. Halasz, G. G. Z. Zhang, J. R. G. Sander, D. G. Reid, L. R. MacGillivray, M. J. Duer and W. Jones, *Chem. Sci.,* 2013, **4**, 4417; (b) N. Schultheiss and A. Newman, *Cryst. Growth Des.,* 2009, **9**, 2950.
2. (a) GRAS Notices: http://www.cfsan.fda.gov/~rdb/opa-gras.html. (b) Food additive status list: http://www.cfsan.fda.gov/~dms/opaappa.html.
3. (a) H. G. Brittain, *Cryst. Growth Des.,* 2012, **12**, 5823; (b) N. J. Babu and A. Nangia, *Cryst. Growth Des.,* 2011, **11**, 2662; (c) R. Thakuria, A. Delori, W. Jones, M. P. Lipert, L. Roy and N. Rodríguez-Hornedo, *Int. J. Pharm.,* 2013, **453**, 101; (d) S. Datta and D. J. W. Grant, *Nat. Rev. Drug Discov.,* 2004, **3**, 42.
4. J. Remenar, S. Morissette, M. Peterson, B. Moulton, J. MacPhee, H. Guzman and Ö. Almarsson, *J. Am. Chem. Soc*., 2003, **125**, 8456.
5. S. L. Childs, L. J. Chyall, J. T. Dunlap, V. N. Smolenskaya, B. C. Stahly and G. P. Stahly, *J. Am. Chem. Soc.,* 2004, **126**, 13335.

6. (a) A. V. Trask, W. D. S. Motherwell and W. Jones, *Cryst. Growth Des.,* 2005, **5**, 1013; (b) W. T. A. Harrison, H. S. Yathirajan, S. Bindya, H. G. Anilkumar and Devaraju, *Acta Crystallogr., Cryst. Struct. Commun.*, 2007, C**63**, 129; (c) G. Petruševski, P. Naumov, G. Jovanovski and S. Ng. Weng, *Inorg. Chem. Commun.,* 2008, **11**, 81; (d) M. Cheney, D. Weyna, N. Shan, M. Hanna, L. Wojtas and M. Zaworotko, *J. Pharm. Sci.*, 2011, **100**, 2172.

7. (a) J. A. Como and W. E. Dismukes, *N. Engl. J. Med.*, 1994, **330**, 263; (b) S. Tsutsumi, M. Iida, N. Tada, T. Kojima, Y. Ikeda, T. Moriwaki, K. Higashi, K. Moribe and K. Yamamoto, *Int. J. Pharm.,* 2011, **421**, 230.

8. (a) Nonappa, M. Lahtinen, E. Kolehmainen, J. Haarala and A. Shevchenko, *Cryst. Growth Des.,* 2013, **13**, 346; (b) A. Shevchenko, L. Bimbo, I. Miroshnyk, J. Haarala, K. Jelínková, K. Syrjänen, B. van Veen, J. Kiesvaara, H. Santos and J. Yliruusi, *Int. J. Pharm.,* 2012, **436**, 403; (c) J. Kastelic, Ž. Hodnik, P. Šket, J. Plavec, N. Lah, I. Leban, M. Pajk, O. Planinšek and D. Kikelj, *Cryst. Growth Des.,* 2010, **10,** 4943; (d) J. Kastelic, N. Lah, D. Kikelj and I. Leban*, Acta Crystallogr., Crystal Struct. Commun.*, 2011, C**67**, 370; (e) J. Kastelic, D. Kikelj, I. Leban and N. Lah, *Acta Crystallogr., Sec. E: Struct. Reports Online*, 2013, **E69**, 0378; (f) M. Caira, K. Alkhamis and R. Obaidat, *J. Pharm. Sci.,* 2004, **93**, 601; (g) Y. Ling, L. Zhang, J. Li, S.-S. Fan and M. Du, *CrystEngComm*, 2010, **12**, 604; (h) Y. Ling, L. Zhang, J. Li and A. X. Hu, *Cryst. Growth Des.,* 2009, **9**, 2043.

9. (a) K. Ravikumar, B. Sridhar, K. Prasad and A. Bhujanga Rao, *Acta Crystallogr., Struct. Reports Online*, 2007, E**63**, 565; (b) R. P. Dickinson, A. S. Bell, C. A. Hitchcock, S. Narayanaswami, S. J. Ray, K. Richardson and P. F. Troke, *Bioorg. Med. Chem. Lett.,* 1996, **6**, 2031; (c) L. J. Taylor, D. G. Papadopoulos, P. J. Dunn, A. C. Bentham, N. J. Dawson, J. C. Mitchell and M. J. Snowden, *Org. Process. Res. Dev.*, 2004, **8**, 674.

10. (a) S. Roffey, S. Cole, P. Comby, D. Gibson, S. Jezequel, A. Nedderman, D. Smith, D. Walker and N. Wood, *Drug Metab. Dispos.,* 2003, **31**, 731; (b) P. Colomer, M. Lloret and S. Pérez, *European Patent Application* 10382204.5, EP2409699 **A1**, 2012; (c) B. Zaludek and L. Zatloukalova, PCT/EP2011/059945, WO2012171561 **A1**, 2012.

11. (a) B. Sarma, N. K. Nath, B. R. Bhogala and A. Nangia, *Cryst. Growth Des.,* 2009, **9**, 1546; (b) B. Sarma, R. Thakuria, N. K. Nath and A. Nangia, *CrystEngComm*, 2011, **13**,

3232; (c) S. L. Johnson and K. A. Rumon, *J. Phys. Chem.,* 1965, **69**, 74; (d) S. L. Childs, G. P. Stahly and A. Park, *Mol. Pharm.,* 2007, **4**, 323.

12. (a) M. C. Etter, *J. Phys. Chem.* 1991, **95**, 4601; (b) M. C. Etter, *Acc. Chem. Res.,* 1990, **23**, 120; (c) J. Grell, J. Bernstein and G. Tinhofer, *Acta Crystallogr., Struct. Sci.,* 1999, B**55**, 1030.
13. (a) C. M. Buchanan, N. L. Buchanan, K. J. Edgar and M. G. Ramsey, *Cellulose*, 2007, **14**, 35; (b) G. N. K. Reddy, V. V. S. R. Prasad, N. Devanna and P. K. Maharana *Der Pharmacia Letter,* 2011, **3**, 249; (c) C. A. Hollingsworth, P. G. Seybold and C. M. Hadad *Int. J. Quantum Chem.,* 2002, **90**, 1396; (d) J. C. R. Corrêa, C. D. Vianna-Soares and H. R. N. Salgado, *Chromat. Res. Int.*, doi:10.1155/2012/610427.
14. (a) N. K. Nath and A. Nangia, *Cryst. Growth Des.,* 2012*,* **12***,* 5411; (b**)** N. K. Nath, B. K. Saha and A. Nangia, *New J. Chem.,* 2008, **32**, 1693; (c) S. K. Chandran, R. Thakuria and A. Nangia, *CrystEngComm*, 2008, **10**, 1891*;* (d*)* R. Thakuria and A. Nangia, *Cryst. Growth Des.,* 2013, **13**, 3672; (e) M. R. Edwards, W. Jones and W.D. S. Motherwell, *CrystEngComm,* 2006**,** **8***,* 545; (f) D. Cinčić, T. Friščić and W. Jones, *New J. Chem.,* 2008, **32**, 1776; (g) A. Kalman, L. Parkanyi and G. Aragay*, Acta Crystallogr., Struct. Sci.*, 1993, B**49**, 1039; (h) A. Anthony, M. Jaskolski, A. Nangia and G. R. Desiraju, *Chem. Commun.,* 1998, 2537.
15. (a) T. Gelbrich and M. B. Hursthouse, *CrystEngComm*, 2005, **7**, 324; (b) T. Gelbrich and M. B. Hursthouse, *CrystEngComm*, 2006, **8**, 448; (c) T. Gelbrich, T. L. Threlfall and M. B. Hursthouse, *CrystEngComm*, 2012, **14**, 5454.
16. (a) Cambridge Structural Database, ver. 5.34, ConQuest 1.15, November 2012 release, May 2013 update, Cambridge Crystallographic Data Center, www.ccdc.cam.ac.uk; (b) A. Newman, *Org. Process. Res. Devel.*, 2013, **17**, 457; (c) M. R. Chierotti and R. Gobetto *CrystEngComm,* 2013, **15**, 8599; (d) T. Pawlak, P. Paluch, K. Trzeciak-Karlikowska, A. Jeziorna and M. J. Potrzebowski *CrystEngComm,* 2013, **15**, 8680; (e) B. A. Zakharov, E. A. Losev and E. V. Boldyreva, *CrystEngComm,* 2013, **15**, 1693.
17. P. Vishweshwar, A. Nangia and V. M. Lynch*, Cryst. Growth Des.,* 2003, **3**, 783.
18. (a) M. K. Mishra, S. Varughese, U. Ramamurty and G. Desiraju*, J. Am. Chem. Soc.,* 2013*,* **135,** 8121; (b) S. Bhattacharya, V. G. Saraswatula and B. K. Saha, *Cryst. Growth Des.*, 2013, **13**, 3299.

19. (a) S. M. Berge, L. D. Bighley and D. C. Monkhouse, *J. Pharm. Sci.*, 1977, **66**, 1; (b) C. L. Cooke and R. Davey, *Cryst. Growth Des.*, 2008, **8**, 3483; (c) M. Hawley and W. Morozowich, *Mol. Pharm.*, 2010, **7**, 1441; (d) R. Thakuria and A. Nangia, *CrystEngComm*, 2011, **13**, 1759.

20. (a) D. J. Good and N. Rodríguez-Hornedo, *Cryst. Growth Des.*, 2009, **9**, 2252; (b) S. L. Childs, N. Rodríguez-Hornedo, L. S. Reddy, A. Jayasankar, C. Maheshwari, L. McCausland, R. Shipplett and B. C. Stahly, *CrystEngComm*, 2008, **10**, 856; (c) A. T. M. Serajuddin, *Adv. Drug Deliv. Rev.,* 2007, **59**, 603; (d) B. D. Anderson and R. A. Conradi, *J. Pharm. Sci.*, 1985, **74**, 815.

21. (a) C. V. S. Subrahmanyam, *Textbook Of Biopharmaceutics & Pharmacokinetics, Concepts & Applications*, 1st Ed., M. K. Jain Vallabh Prakashan, **2010**; (b) Y. Qiu, Y. Chen, L. Liu and G. G. Z. Zhang, *Developing Solid Oral Dosage Forms: Pharmaceutical Theory and Practice*, 1st Ed., Academic Press, **2009**, pp. 75–86; (c) M. Abraham, A. Ibrahim, A. Zissimos, Y. Zhao, J. Comer and D. Reynolds, *Drug Discov. Today*, 2002, **7**, 1056; (d) H. van De Waterbeemd, D. Smith, K. Beaumont and D. Walker, *J. Med. Chem.*, 2001, **44**, 1313.

22. (a) SAINT-Plus, version 6.45; Bruker AXS Inc., Madison, WI, 2003.(b) G. M. Sheldrick, SADABS, Program for Empirical Absorption Correction of Area Detector Data; University of Goettingen, Germany, 1997. (c) SMART, version 5.625 and SHELX-TL, version 6.12; Bruker AXS Inc.: Madison, Wisconsin, USA, 2000. (d) Oxford Diffraction. CrysAlis CCD and CrysAlis RED, versions 1.171.33.55; Oxford Diffraction Ltd: Yarnton, Oxfordshire, UK, 2008. (e) Dolomanov, O. V.; Bourhis, L. J.; Gildea, R. J.; Howard, J. A. K.; Puschmann, H. OLEX2: A complete structure solution, refinement and analysis program. *J. Appl. Crystallogr.* 2009, **42**, 339. (f) Spek, A. L. PLATON, A Multipurpose Crystallographic Tool; Utrecht University: Utrecht, Netherlands, 2002. A. L. Spek, Single- crystal Structure Validation with the Program PLATON. *J. Appl. Crystallogr.* 2003, **36**, 7; (g) L. J. Barbour, X-Seed, Graphical Interface to SHELX-97 and POV-Ray; University of Missouri—Columbia, 1999. (h) N. Kraus, G. Nolze, Powder Cell, version 2.3, A Program for Structure Visualization, Powder Pattern Calculation and Profile Fitting; Federal Institute for Materials Research and Testing: Berlin, Germany, 2000.

Graphical abstract

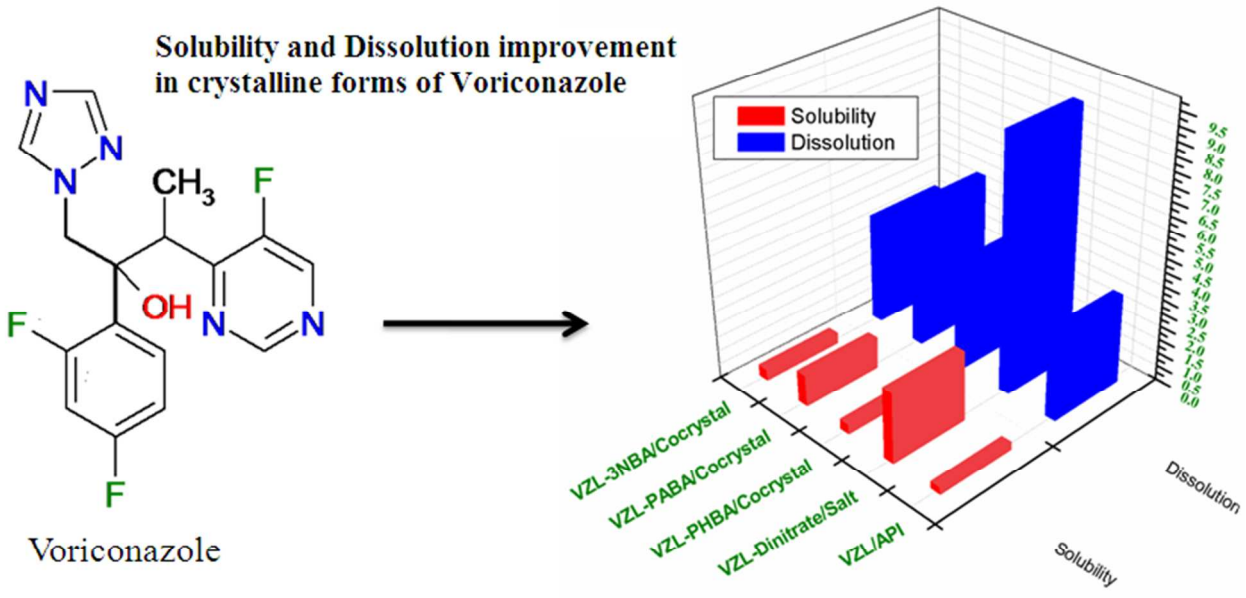

Novel crystalline forms of Voriconazole drug are identified with improved aqueous solubility. The dinitrate salt of voriconazole exhibited 10 fold higher solubility and 3 times faster dissolution rate in 0.1 N HCl medium compared to the reference drug.